

## Physics Contribution

# Quality Control of High-Dose-Rate Brachytherapy: Treatment Delivery Analysis Using Statistical Process Control

Charles M. Able, MS, Megan Bright, MS, and Bart Frizzell, MD

*Department of Radiation Oncology, Wake Forest School of Medicine, Winston-Salem, North Carolina*

Received Nov 20, 2010, and in revised form Apr 2, 2012. Accepted for publication May 8, 2012

### Summary

This study investigated the application of a quality control methodology, statistical process control, to evaluate the proper operation of high-dose-rate brachytherapy. Evaluation of the treatment delivery process may be superior to the current paradigm of quality assurance of individual system components. Results suggest that inclusion of a statistical process control evaluation prior to treatment can detect errors in the treatment planning and delivery process.

**Purpose:** Statistical process control (SPC) is a quality control method used to ensure that a process is well controlled and operates with little variation. This study determined whether SPC was a viable technique for evaluating the proper operation of a high-dose-rate (HDR) brachytherapy treatment delivery system.

**Methods and Materials:** A surrogate prostate patient was developed using Vyse ordnance gelatin. A total of 10 metal oxide semiconductor field-effect transistors (MOSFETs) were placed from prostate base to apex. Computed tomography guidance was used to accurately position the first detector in each train at the base. The plan consisted of 12 needles with 129 dwell positions delivering a prescribed peripheral dose of 200 cGy. Sixteen accurate treatment trials were delivered as planned. Subsequently, a number of treatments were delivered with errors introduced, including wrong patient, wrong source calibration, wrong connection sequence, single needle displaced inferiorly 5 mm, and entire implant displaced 2 mm and 4 mm inferiorly. Two process behavior charts (PBC), an individual and a moving range chart, were developed for each dosimeter location.

**Results:** There were 4 false positives resulting from 160 measurements from 16 accurately delivered treatments. For the inaccurately delivered treatments, the PBC indicated that measurements made at the periphery and apex (regions of high-dose gradient) were much more sensitive to treatment delivery errors. All errors introduced were correctly identified by either the individual or the moving range PBC in the apex region. Measurements at the urethra and base were less sensitive to errors.

**Conclusions:** SPC is a viable method for assessing the quality of HDR treatment delivery. Further development is necessary to determine the most effective dose sampling, to ensure reproducible evaluation of treatment delivery accuracy. © 2013 Elsevier Inc.

## Introduction

Statistical process control (SPC) was developed by Walter A. Shewhart nearly a century ago (1). As an employee of Bell

Telephone Laboratories, Shewhart used SPC to address quality issues in industry. He accomplished this by applying statistics to determine whether processes exhibited controlled behavior. At the core of SPC lies what are called process behavior charts (PBC), which are graphs containing data from a chosen process. The

Reprint requests to: Charles M. Able, MS, Assistant Professor, Department of Radiation Oncology, Wake Forest School of Medicine,

Medical Center Boulevard, Winston Salem, North Carolina 27157. Tel: (336) 878-6036; Fax: (336) 878-6704; E-mail: [cable@wfulmc.edu](mailto:cable@wfulmc.edu)  
Conflict of interest: none.

action limits of these graphs are derived from the historical average and average range. If every data point lies within the action limits, we can generally assume that the process is stable, with little variation, as long as the limits themselves do not have a large spread. Therefore, SPC facilitates the characterization and control of a process using probability and statistics as a data-driven graphical tool. A number of studies have applied SPC to different facets of radiation therapy, but there have been no studies applying SPC to brachytherapy procedures (2-7).

High-dose-rate (HDR) brachytherapy is a complex procedure within the radiation oncology discipline. The potential for error is relatively high due to the many individual tasks which must be interwoven into a team approach for successful treatment delivery. The placement of applicators, followed by radiographic imaging (computed tomography [CT], fluoroscopy, and others), image-based treatment planning, and finally implementation of treatment delivery through the remote after-loading unit (RAU) is obviously a complex process. The recommended quality assurance (QA) procedures for HDR brachytherapy are numerous (8, 9), but they test only whether individual aspects of HDR brachytherapy treatment (source strength, catheter length, and other factors) are within set tolerance values. In a new approach to radiation therapy QA, SPC tests the processes themselves to determine if they are stable, with little variation. The aim of this study was to investigate whether SPC is a viable technique for evaluating the proper operation of an HDR brachytherapy treatment delivery system.

## Methods and Materials

Metal oxide semiconductor field-effect transistors (MOSFETs) were first calibrated in a customized jig to obtain a calibration factor for Ir-192 in water. Next, a customized anatomically correct, water-equivalent phantom was created for HDR treatment delivery. Treatment plans were created using a commercial treatment planning system and delivered with an HDR RAU. After a series of accurate plan deliveries were completed, we modified several parameters to intentionally introduce operational and treatment delivery errors. The accurately delivered treatment measurement results were used to create action limits using SPC methodology. We then tested the hypothesis that SPC was sensitive enough to detect errors in clinical treatment delivery.

### MOSFET calibration

The PTW N30002 model chamber (PTW Freiburg, Breisgau, Germany), electrometer (Cardinal Health Therapy Cardinal Health, Dublin, Ohio) and Thomson & Nielsen MOSFET dosimetry system were used to calibrate 10 MOSFETs (model 502RD, Best Medical, Ottawa, Canada). To aid in the calibration of the MOSFETs and the dose verification via ion chamber, we created a custom-made polystyrene support stand by which the Ir-192 HDR source could be positioned accurately with respect to the detectors (Fig. 1). MOSFETs were calibrated against a Farmer-type ionization chamber with calibration factors traceable to the national standard at distances of 4.9 cm and 1.6 cm from the Ir-192 source in the water phantom. All calibration measurements were performed within an estimated positioning uncertainty of 1 mm.

The ion chamber calibration factor for Ir-192 was derived, using the processes reported by Reynaert et al (10) and Tolli et al

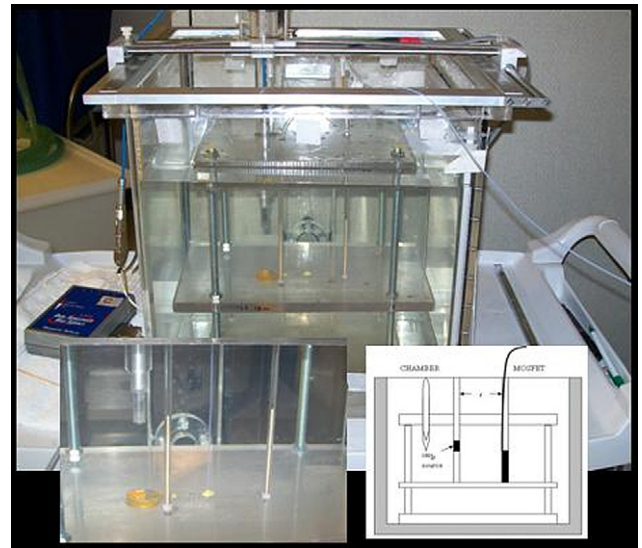


**Fig. 1.** Custom-made polystyrene MOSFET and ion chamber calibration support stand allowed the Ir-192 HDR source to be positioned accurately with respect to the detectors. The support stand is submerged in a water phantom to obtain full scatter conditions during the dose calibration.

(11), from the absorbed dose to water cobalt-60 calibration factor ( $N_{D,w}$ ) obtained from an accredited dosimetry calibration laboratory.

$$D_{w, Ir-192} = N_K (M * C_{TP}) CF_H \tag{1}$$

where  $CF_H = (N_d/N_K) * [(S/\rho)^{Water} / (S/\rho)^{Air}] * P_{wall} * P_{cel} * P_d * P_n$  for further clarification

$$N_d = N_{gas} = N_{D,w} * A_{ion} * A_{repl} / \left\{ \left[ (L/\rho)^{Graphite} / (L/\rho)^{Air} \right] * \left[ (\mu_{en}/\rho)^{water} / (\mu_{en}/\rho)^{Graphite} \right] \right\}$$

and  $N_K$  is the air kerma calibration factor.

For additional details and definitions, the reader is referred to American Association of Physicists in Medicine (AAPM) Task Group 21 Report (12).

### Phantom development

A surrogate patient consisting of anatomically correct prostate, bladder, rectum, and urethra was developed using Vyse ordnance gelatin, known for its quality in simulating human tissue. Research has been done in the fields of wound ballistics and forensic pathology to verify tissue equivalence (13). The mixture was distributed into 3 molds so that organ structures could be fabricated. The prostatic urethra was represented by plastic tubing (5 mm outer diameter). Once the structures were completed, they were covered with a thin layer of petroleum jelly to provide delineation during CT imaging. Small plastic tubes (3 mm outer diameter) were placed around the periphery of the prostate structure to later hold the MOSFETs. The bladder, prostate, and rectum were positioned in a separate mold in proper relative proximity according to human anatomy. Additional gelatin mixture was poured around the structures to develop a complete surrogate patient phantom.

## Needle and MOSFET placement

The radiation oncologist performed the needle placement according to our clinical protocol. HDR needles (typically, 12-14) are positioned in a standard distribution depending on the size of the prostate. During the phantom implantation procedure, 12 interstitial stainless steel needles (18 gauge, 20 cm) were inserted into the prostate under ultrasonographic guidance. The prostate template was sutured to the Plexiglas opening to help ensure stability of needle placement. Reference marks were drawn on needles at template level, and the distance from the template to the needle hub was recorded to allow accurate repositioning when necessary.

A CT scan was acquired to validate needle position so MOSFETs could be placed. A detector train of 3 MOSFETs was inserted into each of the detector holders. MOSFETs were spaced 2.5 cm apart and bonded together using cyanoacrylate (Super Glue). Under CT guidance, the MOSFETs were positioned such that the distal MOSFET in each tube was geographically at the base of the prostate. Figure 2 shows a transverse cross-section of the relative positions of the needles and detectors. A final CT dataset was acquired for treatment planning purposes. This information was transferred to the Varian BrachyVision (version 8.1.20) planning workstation.

## Treatment planning

Treatment planning was performed according to our clinical protocol for prostate HDR Ir-192 brachytherapy patients. All relevant structures are delineated (prostate, bladder, urethra, and rectum). A planning target volume ( $106 \text{ cm}^3$ ) was created from the prostate ( $67 \text{ cm}^3$ ), using our typical margins (ie, 3 mm lateral and anterior, 0 mm posterior, and 5 mm cephalad and caudad). Evaluation of the CT dataset confirmed the gelatin average attenuation coefficient was within 2% of water. All dose calculations assumed the medium was water. Each MOSFET was individually contoured

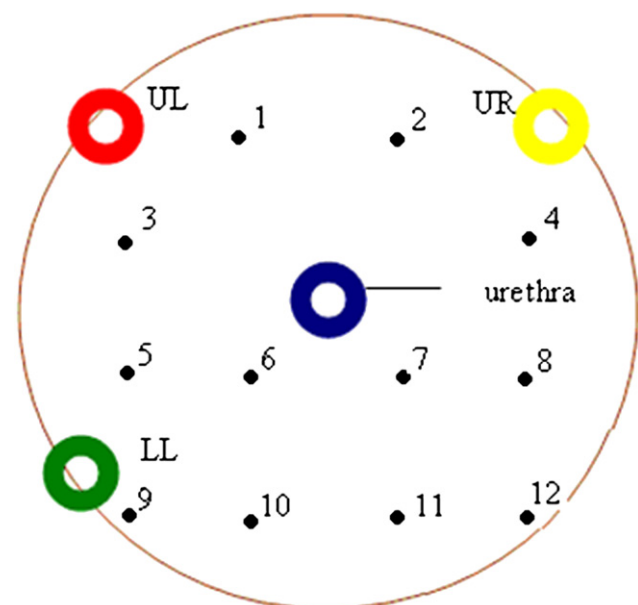


**Fig. 2.** Transverse plane view of MOSFET detector train positions (colored circles) and HDR needle positions (black circles) in the prostate.

to allow us to determine the dose to each location. Needles were defined, and a dose of 200 cGy was prescribed to allow repeated treatment delivery without reaching the dose saturation level of the MOSFET detectors. Geometric optimization was performed, followed by a manual optimization to further improve dose uniformity. Final plans were reviewed and approved by the radiation oncologist. In summary, the plan consisted of 12 needles with 129 dwell positions spaced 0.5 cm apart, delivering a prescribed peripheral dose of 200 cGy (Fig. 3).

## Treatment delivery

Sixteen accurately delivered HDR treatments ( $t$ ) were given to the phantom, containing 10 MOSFETs, for a total of 160 data points. The mV reading from each MOSFET was converted to dose, using its calibration factor determined at 1.6 cm from the HDR source. Means and standard deviations of the mean were calculated for each detector location. These measured values were used to determine the SPC action lines or limits. Afterward, a number of errors were introduced to see if they could be detected by the SPC limits. These errors included wrong patient (one patient's plan used for a different patient), wrong source calibration (3- and 7-day source decay inaccuracy, resulting in  $-2.78\%$  and  $-6.36\%$  dose underestimations, respectively), wrong sequence (2 needles, no. 6 and no. 10, switched in location on turret), single needle displaced inferiorly  $5 \pm 1 \text{ mm}$  (no. 1 needle), and entire implant displaced inferiorly ( $2 \pm 1 \text{ mm}$  and  $4 \pm 1 \text{ mm}$ ). Any shifts of needle positions were done so by hand according to the reference marks previously placed on the needles and ruler measurements from the template to the needle's hub.

## Process behavior charts

To monitor a process, typically 2 PBCs are created: a mean chart for sample or subgroup means,  $\bar{X}$ , and a range chart for sample

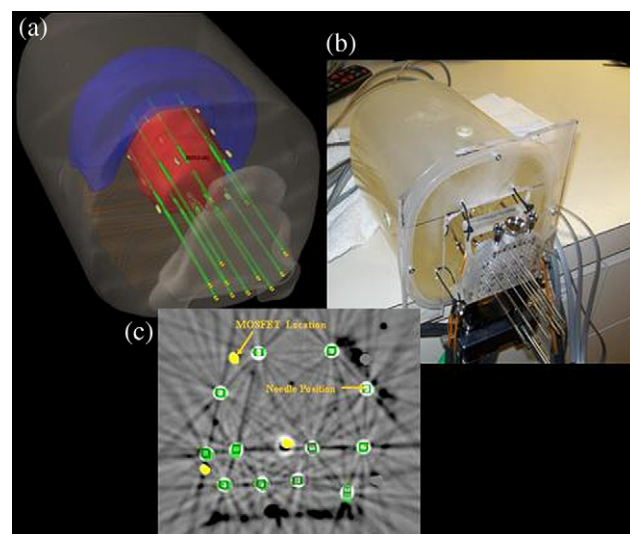


**Fig. 3.** Image collage of (clockwise order) (a) 3-dimensional computer model of prostate phantom, (b) gelatin prostate phantom with needles and detectors in treatment delivery position, and (c) transverse plane CT graphic of needle and detector locations.

or subgroup ranges, *R*. Each MOSFET constituted a subgroup of size *n*=1. Because the subgroup size is 1, individual (I) and moving range (MR) PBCs were used in our evaluation (14, 15). Individual PBC limits were created by simply calculating the mean dose for each MOSFET location.

$$I_c = \bar{X} = \left[ \left( \sum_{t=1, \dots, T} I_t \right) / T \right] \tag{2}$$

where *T* is 16 and *I<sub>t</sub>* is the accurately delivered dose for treatment number (*t*) for a single MOSFET.

MR values were determined by calculating the difference between sequential measurements. MR limits were calculated using the numerical average of the MR values.

$$MR_t = |I_t - I_{t+1}| \tag{3}$$

$$MR_c = \overline{MR} = \left[ \left( \sum_{t=1, \dots, T-1} MR_t \right) / T - 1 \right] \tag{4}$$

where *T* = 16 and *MR<sub>t</sub>* = dose range of accurately delivered treatment number (*t*) for a single MOSFET.

The centerline for the subgroup I chart is *I<sub>c</sub>*, which is the process or grand mean of all subgroup I values. The centerline for the range chart is *MR<sub>c</sub>*, which is the mean of all subgroup MR values. The I chart will have an upper action line (*I<sub>u</sub>*), a centerline (*I<sub>c</sub>*), and a lower action line (*I<sub>l</sub>*) (1, 16, 17), defined as

$$I_u = \bar{X} + 3 \frac{\overline{MR}}{d_2 \sqrt{n}} = UAL \tag{5}$$

$$I_c = \bar{X}$$

$$I_l = \bar{X} - 3 \frac{\overline{MR}}{d_2 \sqrt{n}} = LAL$$

where the factor 3 is representative of the number of standard deviations from the mean that creates the margin for standard action lines or limits. Similarly, the R chart will have an upper action line (*MR<sub>u</sub>*), a centerline (*MR<sub>c</sub>*), and lower action line (*MR<sub>l</sub>*), defined as

$$MR_u = \left( 1 + 3 \frac{d_3}{d_2} \right) \overline{MR} = UAL \tag{6}$$

$$MR_c = \overline{MR}$$

$$MR_l = \left( 1 - 3 \frac{d_3}{d_2} \right) \overline{MR} = LAL$$

Quantities *d<sub>2</sub>* and *d<sub>3</sub>* are correction factors that reflect the non-normality of the distribution of *R* values and also depend on the subgroup size *n* (18). The MR limits have an asymmetrical distribution about the mean MR because the range is a positively skewed value and cannot be less than zero.

It is important to note that the AAPM Task Group 138 report explicitly recommends the use of the coverage factor of 2 standard deviations from the mean for dosimetric uncertainties in brachytherapy (19). The factor of 3 used in Eqs. 5 and 6 is an appropriate factor in SPC analysis of the treatment delivery process. It is considered an economical factor balancing the cost of intervention for a type 1 error (a signal indicating an alarm incorrectly) versus the clinical implications of a type 2 error (a signal indicating there is no alarm when in fact a problem exists) (14, 16). The implication of exceeding the mean or R chart limits for the process is thoroughly presented in SPC literature (1, 14-18), and an extensive review is beyond the scope of this work. Generally, changes

identified in mean values can be investigated for nonrandom causes prior to the process reaching an uncontrolled state. The range chart is capable only of identifying whether a process is controlled or uncontrolled (14, 15).

The MR values for treatments with an error introduced (*MR<sub>e</sub>*) were calculated using the equation

$$MR_e = |\bar{X} - I_e| \tag{7}$$

where *I<sub>e</sub>* = dose measured for a treatment with a single error introduced for a single MOSFET.

An I and an MR PBC was created for each MOSFET location. Each PBC contains 2 data sets: accurately delivered treatments (data set 1) and treatments delivered with an error introduced (data set 2). Results of data set 1 provide an evaluation of the performance of the process as these data were used to create the process limits. Results of data set 2 provide (1) a determination of the effectiveness of SPC to accurately detect treatment delivery errors, (2) the overall impact of specific treatment delivery errors on the accuracy of the treatment, (3) the sensitivity of different implant regions to different treatment delivery errors, and (4) guidance on the location of dose delivery sampling to reproducibly detect treatment delivery errors. Table 1 shows measurement data points. Measurement number 18-28 constitutes data set 2, treatment deliveries with an error introduced.

## Results

A dose of 100 cGy was delivered to the ion chamber at distances of 1.6 cm and 4.9 cm. The dose measured using the ion chamber system was 102.6 ± 0.1 cGy and 101.0 ± 0.1 cGy, respectively. This was clearly in excellent agreement. MOSFETs were then calibrated at 1.6 cm and 4.9 cm. We chose to use the calibration factors at 1.6 cm to evaluate the dose delivered during the prostate HDR treatment. This decision was made because the dose contribution to each MOSFET was greater from those dwell positions that were in close proximity (<2.0 cm) and resulted in more accurate dose calculations. The mean dose and standard deviation of the mean for each detector location is displayed in Table 2.

We found that the PBCs are more easily analyzed when grouped by prostate anatomical location (ie, apex, mid-gland, and base). Each anatomical location is then characterized by the PBC for several geographical positions: lower left (LL), upper left, upper right, and/or urethra. Figure 4 is one example of a PBC for the LL apex location of the prostate.

**Table 1** PBC data legend

Measurement	HDR treatment delivery
1-16 (data set 1)	Accurately delivered treatments
18	Wrong patient
19	Wrong source calibration (3 d)
20	Wrong source calibration (7 d)
21-22	Wrong sequence (no. 6 and no. 10 were switched)
23-24	No. 1 catheter was displaced 5 mm inferiorly
25-26	Entire implant was displaced 2 mm inferiorly
27-28	Entire implant was displaced 4 mm inferiorly

**Table 2** Accurate treatment delivery

MOSFET location	Mean measured dose (cGy)	Standard deviation of mean (cGy)	Standard deviation of mean (%)
1) Upper right—apex	225.25	3.6	1.6
2) Upper left—base	184.44	4.0	2.2
3) Urethra—base	214.70	4.1	1.9
4) Urethra—mid-gland	231.15	4.2	1.8
5) Urethra—apex	163.07	3.4	2.1
6) Lower left—base	202.84	6.6	3.2
7) Lower left—mid-gland	290.41	3.1	1.1
8) Lower left—apex	216.18	3.8	1.8
9) Upper left—mid-gland	235.13	3.7	1.6
10) Upper left—apex	252.63	4.9	1.9

## Error detection

Review of these data revealed the following general observations: (1) The PBCs were able to detect all errors introduced in at least 1 of the detection locations. (2) The apex of the prostate was clearly the region most sensitive to all treatment errors introduced. (3) Positional errors were most easily detected at the base and apex of the prostate. Mid-gland typically has the most robust dose and would therefore be less affected by small shifts in dwell position. (4) Small errors in source calibration (3 days) were difficult to detect. (5) The most consistent errors detected were wrong patient plan delivered and large error in source calibration (7 days). (6) False-positive results were seen in data from the base and apex but not from mid-gland. There were 4 false positives (2.5%) resulting from the total number of data points (160) of data set 1.

## Discussion

Overall, this study continues to build upon the foundations of current SPC knowledge and HDR QA. Our results demonstrate SPC can consistently detect large critical errors, wrong patient plan and wrong source calibration, which can impact clinical outcomes and patient safety. Delivery of a standard volumetric treatment and SPC analysis prior to patient treatment can help minimize large errors. It is important to know not only that the treatment delivery process is not controlled but what attribute of the process is uncontrolled. This work was not designed to address this critical aspect. A more detailed systematic analysis is necessary to relate specific treatment delivery errors to demonstrated SPC failure in a particular measurement location.

An interesting result of this study was the relative impact of the different positional errors introduced on dose in specific regions of the implanted volume. One clinical observation of prostate HDR treatment delivery is the superior-inferior displacement of needles due to pelvic pressure and patient positioning. A geographical miss can be detected at the distal end of the implant, demonstrated by the sensitivity of the apex region to the positional errors introduced. Peripheral and centrally located detectors in the mid-gland region were not as sensitive to these errors. A study that correlates the clinical

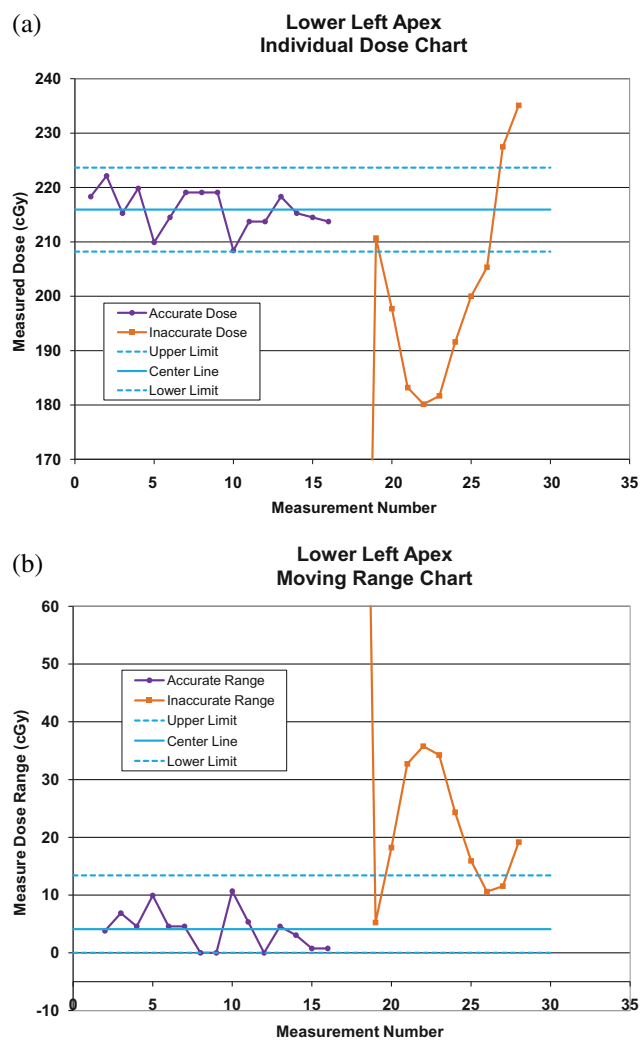


**Fig. 4.** SPC analysis of HDR treatment delivery. I (a) and MR (b) PBCs are shown for LL prostate apex detector location. PBC limits were calculated using the accurate dose delivery data points. Highly deviated inaccurate dose data points (outside graphical range) are not displayed, for better overall graphical clarity.

impact of errors as demonstrated by treatment planning dose-volume histogram analysis to treatment delivery SPC analysis could provide some guidance on SPC action levels as it relates to a medical event.

Clearly, both peripherally and centrally located dose sampling are necessary to detect a wide range of possible treatment delivery errors, beyond what was tested in this study. Our results suggest that peripheral dose sampling in the plane perpendicular to the direction of the applicator and source is critical to detect positional errors resulting from RAU or applicator displacement. Centrally located dose sampling of the delivered treatment can reproducibly detect large errors. While additional tests evaluating the balance between the number and location of dose sampling on the periphery and center will be included in future studies, the current results imply that a 3:1 ratio of peripheral dose sampling to central dose sampling may be adequate to detect both positional and relatively large (>5%) dosimetric calibration errors.

## Clinical QA using SPC

We envision the use of SPC to perform patient-specific QA (PSQA) of the plan, source calibration, and RAU prior to treatment delivery. In the PSQA paradigm, the approved treatment plan is applied to a fixed geometry (phantom) in which an array of embedded solid state dosimeters exist. SPC would be used to evaluate the accuracy of the dose relative to the treatment plan at the central and peripheral dosimeter locations. This would confirm the accuracy and consistency of the treatment process (ie, treatment plan, plan transfer to RAU, source calibration, and operation of RAU). PSQA would significantly alter the current workflow of HDR brachytherapy. Additionally, it has the potential to streamline the current workflow by eliminating some of the standard QA steps. These QA steps could be evaluated only when the PSQA results were outside the action limits.

## Conclusions

QA in HDR brachytherapy prior to daily treatment currently involves verification of the treatment planning dose calculations for adherence to the dose prescription and source calibration. It also includes QA of the treatment delivery device, such as operational checks of all safety systems; presence and operation of emergency equipment; dwell position accuracy at some predetermined distance or series of dwell positions; verification of applicator lengths; and other specific, individual system components. These tests do not inform the clinical team of the accuracy and consistency of the clinical operation of the entire treatment delivery process. This work has demonstrated that SPC methodology has the potential to provide quality control for the clinical treatment delivery process in HDR brachytherapy.

## References

1. Wheeler DJ, Chambers DS. Understanding Statistical Process Control. Knoxville, TN: SPC Press; 1992.

2. Pawlicki T, Whitaker M, Boyer A. Statistical process control for radiotherapy quality assurance. *Med Phys* 2005;32:2777-2786.
3. Gerard K, Grandhaye J, Marchesi V, et al. A comprehensive analysis of the IMRT dose delivery process using statistical process control (SPC). *Med Phys* 2009;36:1275-1285.
4. Basran PS, Woo MK. An analysis of tolerance levels in IMRT quality assurance procedures. *Med Phys* 2008;35:2300-2307.
5. Pawlicki T, Yoo S, Court LE, et al. Moving from IMRT QA measurements toward independent computer calculations using control charts. *Radiother Oncol* 2009;89:330-337.
6. Breen SL, Moseley DJ, Zhang B, et al. Statistical process control for IMRT dosimetric verification. *Med Phys* 2008;35:4417-4425.
7. Able C, Bright M. Quality control of external beam treatment delivery: mechanical parameters. *Med Phys* 2009;36:2428.
8. Kubo HD, Glasgow GP, Pethel TD, et al. High dose-rate brachytherapy treatment delivery: report of the AAPM Radiation Therapy Committee Task Group No. 59. *Med Phys* 1998;25:375-403.
9. Thomadsen BR. Achieving Quality in Brachytherapy. Bristol (UK): Institute of Physics Publishing; 2002.
10. Reynaert N, Verhaegen F, Thierens H. In-water calibration of PDR 192Ir brachytherapy sources with an NE2571 ionization chamber. *Phys Med Biol* 1998;43:2095-2107.
11. Tolli H, Johansson K. Absorbed dose determination at short distance from 60Co and 192Ir brachytherapy sources. *Phys Med Biol* 1998;43:3183-3194.
12. Schulz RJ, Almond PR, Cunningham JR, et al. A protocol for the determination of absorbed dose from high-energy photon and electron beams. *Med Phys* 1983;10:741-771.
13. Fackler ML, Malinowski JA. Ordnance gelatin for ballistic studies. Detrimental effect of excess heat used in gelatin preparation. *Am J Forensic Med Pathol* 1988;9:218-219.
14. Oakland JS. Statistical Process Control. Oxford, UK: Butterworth-Heinemann; 2008.
15. Stapenhurst T. Mastering Statistical Process Control. Oxford, UK: Butterworth-Heinemann; 2005.
16. American Society for Testing and Materials. ASTM Manual on Quality Control of Materials. Philadelphia, PA: American Society for Testing and Materials; 1951.
17. Wheeler DJ. Normality and the Process Control Chart. Knoxville, TN: SPC Press; 2000.
18. Burr IW. The effect of non-normality on constants for Xbar and R charts. In: *Industrial Quality Control*. 1967; 565-569.
19. DeWerd LA, Ibbott GS, Meigooni AS, et al. A dosimetric uncertainty analysis for photon-emitting brachytherapy sources: report of AAPM Task Group No. 138 and GEC-ESTRO. *Med Phys* 2011;38:782-801.